

# 8Be, 12C, 16O, 20Ne, 24Mg, and 32S nuclei and alpha clustering within a generalized liquid drop model

G. Royer, Ramasamy G., P. Eudes

## ► To cite this version:

G. Royer, Ramasamy G., P. Eudes. 8Be, 12C, 16O, 20Ne, 24Mg, and 32S nuclei and alpha clustering within a generalized liquid drop model. F. Cerruti, M. Chadwick, A. Ferrari, T. Kawano, P. Schoofs. 14th Internationale Conference on Nuclear reaction Mechanisms, Jun 2015, Varenna, Italy. CERN, Geneva, 2015, 14th International Conference on Nuclear Reaction Mechanisms Proceedings, 2015-001 (001), pp.71-77, 2015, 14th International Conference on Nuclear Reaction Mechanisms Proceedings. <<https://cds.cern.ch/record/2114737>>. <in2p3-01299744>

**HAL Id: in2p3-01299744**

**<http://hal.in2p3.fr/in2p3-01299744>**

Submitted on 18 Apr 2016

**HAL** is a multi-disciplinary open access archive for the deposit and dissemination of scientific research documents, whether they are published or not. The documents may come from teaching and research institutions in France or abroad, or from public or private research centers.

L'archive ouverte pluridisciplinaire **HAL**, est destinée au dépôt et à la diffusion de documents scientifiques de niveau recherche, publiés ou non, émanant des établissements d'enseignement et de recherche français ou étrangers, des laboratoires publics ou privés.

# $^8\text{Be}$ , $^{12}\text{C}$ , $^{16}\text{O}$ , $^{20}\text{Ne}$ , $^{24}\text{Mg}$ , and $^{32}\text{S}$ nuclei and alpha clustering within a generalized liquid drop model

*G. Royer, G. Ramasamy and P. Eudes*

Laboratoire Subatech, UMR : IN2P3/CNRS-Université-Ecole des Mines, Nantes, France

## Abstract

The potential energy governing the shape and the entrance and decay channels of the  $^{12}\text{C}$ ,  $^{16}\text{O}$ ,  $^{20}\text{Ne}$ ,  $^{24}\text{Mg}$ , and  $^{32}\text{S}$  4n-nuclei has been determined within a generalized liquid drop model. Different three-dimensional and planar shapes have been investigated: linear chain, triangle, square, tetrahedron, pentagon, trigonal bipyramid, square pyramid, hexagon, octahedron, octogon and cube. The rms radii of the linear chains are higher than the experimental rms radii of the ground states. The binding energies of the planar shapes at the contact point are lower than the ones of the three-dimensional configurations. The  $\alpha$  particle plus A-4 daughter configuration leads always to the lowest potential barrier relatively to the sphere configuration.

## 1 Introduction

Hydrogen burning in stars leads to a dense and hot core of helium and to the nucleosynthesis of other nuclei having a possible n- $\alpha$  structure:  $^{16}\text{O}$ ,  $^{20}\text{Ne}$ ,  $^{24}\text{Mg}$ ,  $^{28}\text{Si}$ ,  $^{32}\text{S}$ , ... In these 4n-nuclei the cluster-type states coexist with the mean-field-type states [1]. In  $^{12}\text{C}$  the ground state wave function contains a large amount of  $3\alpha$  cluster wave function. Experimentally, a new high spin  $5^-$  state has been observed recently. It fits well the ground state rotational band of an equilateral triangular spinning top [2]. In  $^{16}\text{O}$  recent calculations lead for the ground state to a tetrahedral configuration of  $\alpha$  particles in agreement with the energy spectrum and with the electromagnetic properties [3, 4] while some excited states are due to the mean-field-type excitation mode while other ones are due to the cluster structure of  $\alpha$ - $^{12}\text{C}$ . In connection with the excited  $0_2^+$  Hoyle state of  $^{12}\text{C}$  and possible excited Hoyle state of  $^{16}\text{O}$ , the  $\alpha$  condensate character of the  $\alpha$ -linear chain has been proposed after comparing a large number of Brink functions with Tohsaki-Horiuchi-Schuck-Röpke wave functions [5, 6].

The generalized liquid drop model (GLDM) previously defined to describe the fission, fusion, ... processes [7–9] has been used to determine the L-dependent potential energy of the following planar or three-dimensional  $\alpha$  clusters: aligned  $\alpha$  chains, isosceles triangle, square, tetrahedron, pentagon, trigonal bipyramid, square pyramid, hexagon, octahedron, octogon and cube.

## 2 Generalized liquid drop model

The GLDM energy is the sum of the volume, surface, Coulomb and proximity energies.

For two separated spherical nuclei :

$$E_V = -15.494 [(1 - 1.8I_1^2)A_1 + (1 - 1.8I_2^2)A_2] \text{ MeV}, \quad (1)$$

$$E_S = 17.9439 [(1 - 2.6I_1^2)A_1^{2/3} + (1 - 2.6I_2^2)A_2^{2/3}] \text{ MeV}, \quad (2)$$

$$E_C = 0.6e^2 Z_1^2/R_1 + 0.6e^2 Z_2^2/R_2 + e^2 Z_1 Z_2/r, \quad (3)$$

where  $I_i$  is the relative neutron excess.

The proximity energy must be added to the surface energy to take into account the effects of the nuclear forces between the surfaces in regard in a gap or a neck between nuclei.

### 3 $^{12}\text{C}$ nucleus

Calculations using Antisymmetrized Molecular Dynamics and Fermionic Molecular Dynamics and without assuming  $\alpha$  clustering led for the different states to triangular  $\alpha$ -configurations with different angles allowing the reproduction of the low-lying spectrum [10, 11]. Using effective field theory and Monte Carlo lattice calculations it has been shown that the  $^{12}\text{C}$  ground state and the first excited state have a compact triangular configuration while the Hoyle state and the second excited state have an obtuse triangular configuration of alpha clusters [12]. These predictions are strengthened by the observation of a new high spin  $5^-$  state at 22.4 MeV compatible with a ground state rotational band of an equilateral triangular spinning top with a  $D_{3h}$  symmetry. Then the Hoyle state is interpreted as the band head of the stretching vibration or breathing mode of this triangular configuration [2].

These oblate ternary configurations have been studied within the GLDM in placing three  $\alpha$  particles at the tops on an isosceles triangle characterized by the angle  $\theta$ . At the contact point the energy of the linear chain of three  $\alpha$  particles ( $\theta=180$  deg.) is higher than the energy of the equilateral triangular shape, the energy difference reaching 7.4 MeV. This is also in favor of an equilateral triangular configuration of the ground state (the energy being almost constant between 120 and 180 degrees). The experimental rms charge radius of the ground state is  $\langle r^2 \rangle^{1/2} = 2.47$  fm. Within the GLDM, at the contact point the rms radius is 2.43 fm for a triangular shape and 3.16 fm for a linear chain. Furthermore the empirical electric quadrupole moment is negative which disagrees with the configuration of three-aligned  $\alpha$  particles for the ground state shape [9].

### 4 $^{16}\text{O}$ nucleus

For the ground state a tetrahedral molecule of alpha particles is predicted [3, 4] and for the first excited

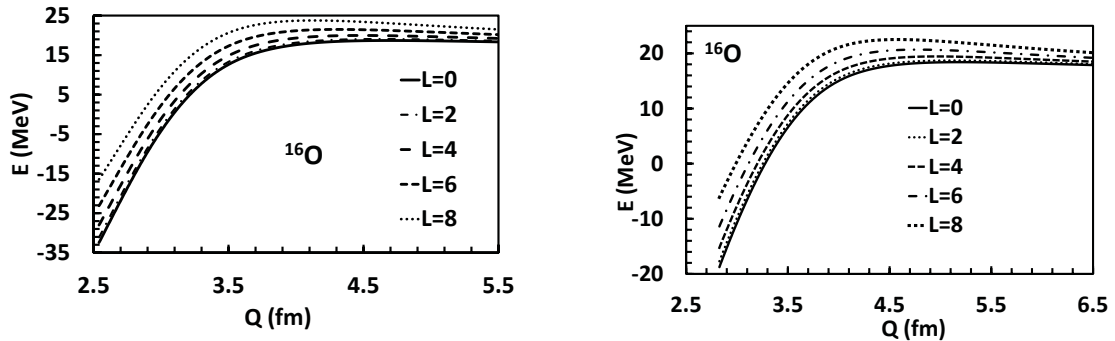


**Fig. 1:** Potential energy of the  $\alpha$ -tetrahedron (left part) and of the  $\alpha$ -square (right part) as functions of the angular momentum (in  $\hbar$  unit) and rms radius.

spin-0 state a square configuration [3]. In Fig. 1 the energies of these two configurations determined from the GLDM are shown. At the contact point between the four spherical  $\alpha$  particles the rms radius is 2.54 fm for a tetrahedron, 2.83 fm for a square and 4.15 fm for a prolate linear chain. Experimentally the rms charge radius of the ground state is  $\langle r^2 \rangle^{1/2} = 2.70$  fm. The ground state has probably not a linear chain configuration. The binding energy is higher for the tetrahedral molecule than for the square shape since for these configurations the proximity energy plays a very important role and the tetrahedron is linked by six bonds and the square by only four bonds. On the contrary, the Coulomb repulsion is lower for the square. The energy difference between the two shapes is 13.7 MeV which is close to  $Q_{d\alpha}$  (14.4 MeV), the energy of the  $0_6^+$  state (15.1 MeV) and 14.0 MeV the energy of a  $0^+$  state. The relative energies at the contact point are respectively 0, 1.3, 4.4, 9.3 and 16 MeV for  $L = 0, 2, 4, 6$  and  $8 \hbar$  for the tetrahedral shape and 0, 1.1, 3.5, 7.4 and 12.6 MeV for  $L = 0, 2, 4, 6$  and  $8 \hbar$  for the square shape.

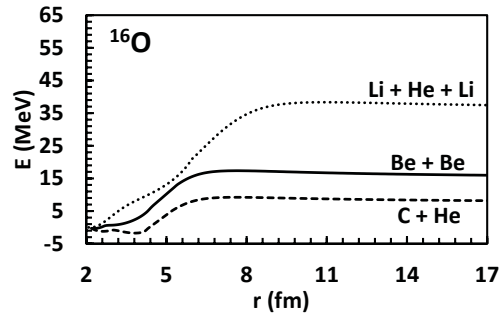


**Fig. 2:** Potential energy governing the  $^{12}\text{C}+^4\text{He}$ ,  $^8\text{Be}+^8\text{Be}$ , and  $^6\text{Li}+^4\text{He}+^6\text{Li}$  nuclear systems versus the distance between the mass centres (at  $L = 0$ ).

The ground state can also be described as double closed shell wave functions but several low-lying excited states are also described within the  $^{12}\text{C}+^4\text{He}$  cluster. The potential energies of the  $^{12}\text{C}+^4\text{He}$ ,  $^8\text{Be}+^8\text{Be}$ , and aligned  $^6\text{Li}+^4\text{He}+^6\text{Li}$  systems have been calculated assuming a spherical shape for the compound nucleus and each nucleus (see Fig. 2). The threshold energies are : 7.2 MeV for  $Q_{\text{He}+^{12}\text{C}}$ , 14.4 for  $Q_{4\alpha}$ , 14.6 for  $Q_{^8\text{Be}+^8\text{Be}}$ , and 35.3 for  $Q_{^6\text{Li}+^4\text{He}+^6\text{Li}}$ . The top of the barriers corresponds to separated nuclei maintained in unstable equilibrium by the balance between the attractive nuclear proximity forces and the repulsive Coulomb forces. Quasimolecular  $^{12}\text{C}+^4\text{He}$  one-body shapes have almost the same energy than the spherical compound nucleus.

## 5 $^{20}\text{Ne}$ nucleus

The trigonal bipyramid, square pyramid and pentagonal molecules have been studied. Their energies are compared in Fig. 3. The rms radius is 2.76 fm for a trigonal bipyramid, 2.79 fm for a square pyramid and 3.29 fm for a pentagon at the contact point. The experimental rms charge radius is  $\langle r^2 \rangle^{1/2} = 3.01$  fm, lower than the rms radius of a prolate linear chain. The binding energy of the trigonal bipyramid is the highest. The number of bonds is five for the pentagon, eight for the square pyramid and nine for the trigonal bipyramid. At the contact point, the energy difference between the trigonal bipyramid and the square pyramid is 21.3 MeV and 15.3 between the square pyramid and the pentagon, while  $Q_{\alpha} = 19.2$  MeV. For the trigonal bipyramid the relative energies to the ground state at the contact point are respectively 0, 1.7, 5.6, 11.7 and 20.1 MeV for  $L = 0, 2, 4, 6$  and  $8 \hbar$ . For the square pyramid the values are 0, 1.0, 3.2, 6.8 and 11.7 MeV for  $L = 0, 2, 4, 6$  and  $8 \hbar$ . For the pentagon it is : 0, 0.6, 2.0, 4.3 and 7.3 MeV for  $L = 0, 2, 4, 6$  and  $8 \hbar$ . Experimentally the energies of the  $2_0^+$  and  $4_0^+$  states are respectively 1.63 and 4.25 MeV.

The ground state band contains the  $^{16}\text{O}+^4\text{He}$  cluster at most 70% and the potential energies of the  $^{16}\text{O}+^4\text{He}$ ,  $^{12}\text{C}+^8\text{Be}$ ,  $^{10}\text{B}+^{10}\text{B}$ , and linear  $^8\text{Be}+^4\text{He}+^8\text{Be}$  systems have been determined assuming spherical shapes for all the nuclei (see Fig. 4). The respective threshold energies are : 4.73 MeV for  $Q_{^{16}\text{O}+^4\text{He}}$ , 11.98 for  $Q_{^8\text{Be}+^{12}\text{C}}$ , 19.35 for  $Q_{^8\text{Be}+^4\text{He}+^8\text{Be}}$ , and 31.14 MeV for  $Q_{^{10}\text{B}+^{10}\text{B}}$ . In the  $^{16}\text{O}+^4\text{He}$  channel quasimolecular one-body shapes have roughly the same energy than the spherical nucleus and the minimum has a cluster structure corresponding to the two  $^4\text{He}$  and  $^{16}\text{O}$  nuclei in contact.

## 6 $^{24}\text{Mg}$ nucleus

The energies of the hexagonal and octahedral  $\alpha$ -molecules are displayed in Fig. 5. The experimental rms charge radius of the ground state is only  $\langle r^2 \rangle^{1/2} = 3.06$  fm. At the contact point the rms radius

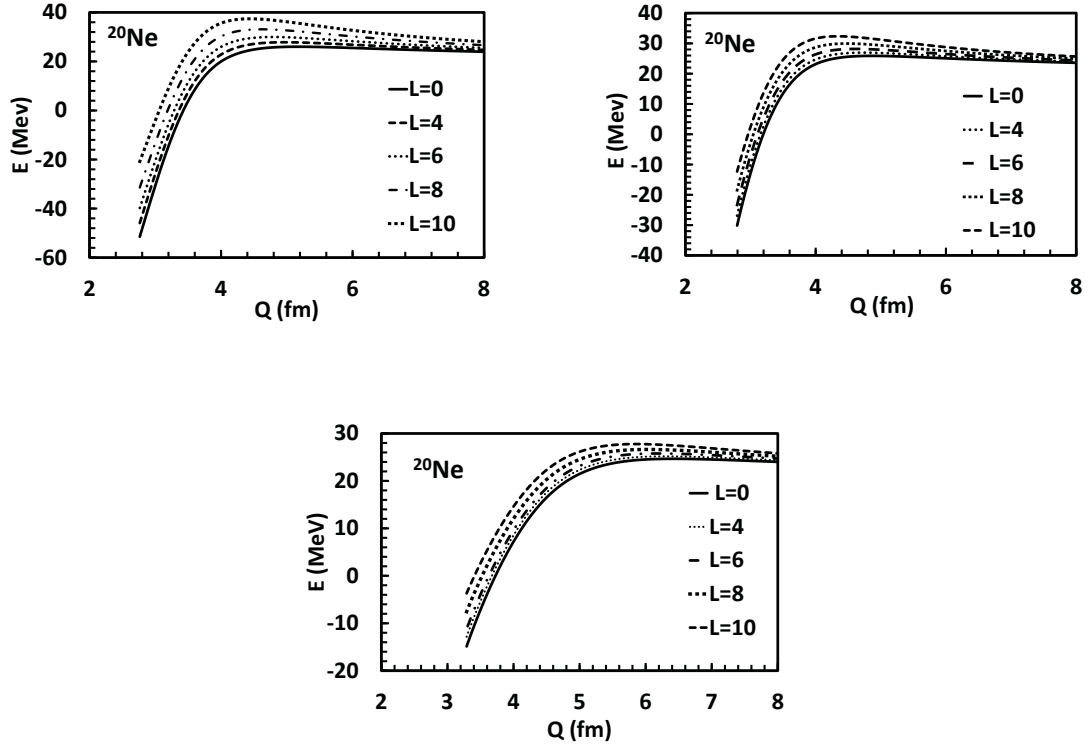


**Fig. 3:** Potential energy of the trigonal bipyramid (on the left), square pyramid (on the right) and the pentagon (on the bottom) as functions of the angular momentum (in  $\hbar$  unit) and rms radius.

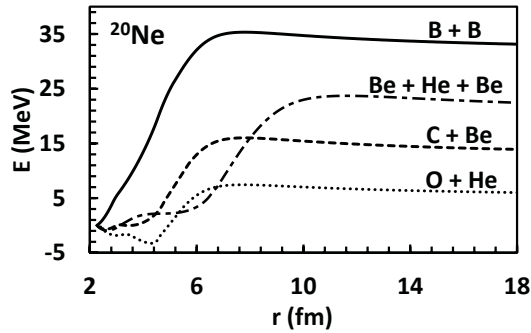


**Fig. 4:** Potential energy governing the  $^{16}\text{O}+^4\text{He}$ ,  $^{12}\text{C}+^8\text{Be}$ ,  $^{10}\text{B}+^{10}\text{B}$ , and linear  $^8\text{Be}+^4\text{He}+^8\text{Be}$  systems versus the distance between the mass centres (at  $L = 0$ ).

is 2.85 fm for an octahedron and 3.79 fm for a hexagon, which excludes the planar shape and the linear chain as possible ground state shapes. The binding energy is higher for the octahedral configuration since there are twelve bonds for the octahedron and only six for the hexagon.

The potential energies of the  $^{16}\text{O}+^8\text{Be}$ ,  $^{12}\text{C}+^{12}\text{C}$ ,  $^8\text{Be}+^8\text{Be}+^8\text{Be}$ , and  $^{10}\text{B}+^4\text{He}+^{10}\text{B}$  systems

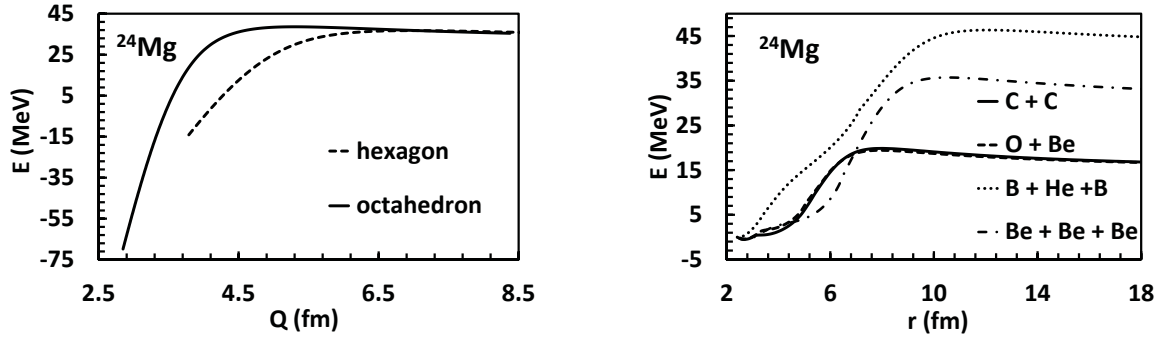


**Fig. 5:** Potential energies of an hexagon and an octahedron from the contact point as a function of the rms radius and potential barriers governing the  $^{16}\text{O}+^8\text{Be}$ ,  $^{12}\text{C}+^{12}\text{C}$ ,  $^8\text{Be}+^8\text{Be}+^8\text{Be}$ , and  $^{10}\text{B}+^4\text{He}+^{10}\text{B}$  reactions versus the distance between the mass centres.

are also shown in Fig. 5. The different  $Q$  values are : 9.32 MeV for  $Q_{^4\text{He}+^{20}\text{Ne}}$ , 13.93 for  $Q_{^{12}\text{C}+^{12}\text{C}}$ , 14.14 for  $Q_{^8\text{Be}+^{16}\text{O}}$ , 28.48 for  $Q_{6\alpha}$ , 28.76 for  $Q_{^8\text{Be}+^8\text{Be}+^8\text{Be}}$ , and 40.46 for  $Q_{^{10}\text{B}+^4\text{He}+^{10}\text{B}}$ .

## 7 $^{32}\text{S}$ nucleus

The octagonal and cubic  $\alpha$ -molecules have been investigated. Their energies are compared in Fig. 6. The experimental rms charge radius is  $\langle r^2 \rangle^{1/2} = 3.26$  fm. The rms radius is 4.85 fm for an octagon and 3.37 fm for a cube at the contact point which seems to exclude the planar and linear configurations. The binding energy is higher for the cubic configuration than for the octogonal shape, indeed there are twelve bonds for the cube and only eight for the octogon.

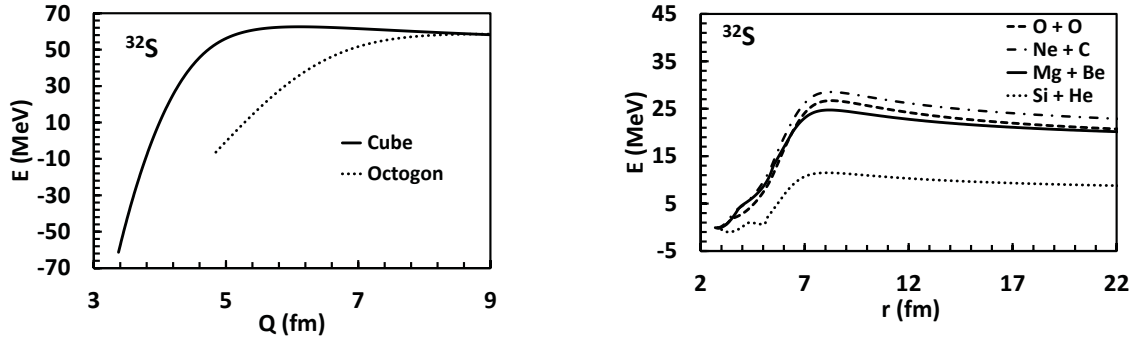


**Fig. 6:** Potential energies of octogonal and cubic molecules from the contact point as a function of the rms radius and potential barriers governing the  $^{28}\text{Si}+^4\text{He}$ ,  $^{24}\text{Mg}+^8\text{Be}$ ,  $^{20}\text{Ne}+^{12}\text{C}$ , and  $^{16}\text{O}+^{16}\text{O}$  systems versus the distance between the mass centres.

The potential energies of the  $^{28}\text{Si}+^4\text{He}$ ,  $^{24}\text{Mg}+^8\text{Be}$ ,  $^{20}\text{Ne}+^{12}\text{C}$ , and  $^{16}\text{O}+^{16}\text{O}$  systems are also given in Fig. 6. The threshold energies are : 6.95 MeV for  $Q_{^4\text{He}+^{28}\text{Si}}$ , 16.54 for  $Q_{^{16}\text{O}+^{16}\text{O}}$ , 17.02 for  $Q_{^8\text{Be}+^{24}\text{Mg}}$ , 18.97 for  $Q_{^{12}\text{C}+^{20}\text{Ne}}$ , 30.96 for  $Q_{^{12}\text{C}+^8\text{Be}+^{12}\text{C}}$ , 34.17 for  $Q_{^{14}\text{N}+^4\text{He}+^{14}\text{N}}$ , and 45.42 for  $Q_{8\alpha}$ . The energy of the  $^{28}\text{Si}+^4\text{He}$  one-body nucleus is relatively constant till the spherical nucleus allowing the cohabitation of different quasimolecular shapes. The superdeformed band contains the

$^{16}\text{O}+^{16}\text{O}$  component by about 44 %.

## 8 Binding energy

The binding energy of these nuclei can be reproduced within the molecular structure picture by summing the binding energy of  $n$  alphas plus the number of bonds multiplied by around 2.4 MeV.

$$\begin{aligned} B(^{12}\text{C}) &= 3 \times B(\alpha) + 3(\text{bonds}) \times 2.42 \text{ MeV}, \\ B(^{16}\text{O}) &= 4 \times B(\alpha) + 6(\text{bonds}) \times 2.41 \text{ MeV}, \\ B(^{20}\text{Ne}) &= 5 \times B(\alpha) + 8(\text{bonds}) \times 2.40 \text{ MeV}, \\ B(^{24}\text{Mg}) &= 6 \times B(\alpha) + 12(\text{bonds}) \times 2.37 \text{ MeV}. \end{aligned} \quad (4)$$

It is difficult to explain this value of 2.4 MeV per bond since it does not correspond to the sum of the mean Coulomb energy and proximity energy by bond.

The binding energy of these nuclei can also be obtained within a core+ $\alpha$  cluster model since this energy is the sum of the binding energies of one alpha and the one of the daughter nucleus plus roughly the Coulomb energy and the proximity energy between the two nuclei.

$$\begin{aligned} B(^{12}\text{C}) &= B(^8\text{Be}) + B(\alpha) + 7.37 \text{ MeV}, \\ B(^{16}\text{O}) &= B(^{12}\text{C}) + B(\alpha) + 7.16 \text{ MeV}, \\ B(^{20}\text{Ne}) &= B(^{16}\text{O}) + B(\alpha) + 4.73 \text{ MeV}, \\ B(^{24}\text{Mg}) &= B(^{20}\text{Ne}) + B(\alpha) + 9.32 \text{ MeV}. \end{aligned} \quad (5)$$

## 9 Conclusion

Within an  $\alpha$ -particle model the energy of the  $^{12}\text{C}$ ,  $^{16}\text{O}$ ,  $^{20}\text{Ne}$ ,  $^{24}\text{Mg}$  and  $^{32}\text{S}$  nuclei has been determined assuming different  $\alpha$ -molecule configurations: linear chain, triangle, square, tetrahedron, pentagon, trigonal bipyramid, square pyramid, hexagon, octahedron, octogon, and cube. Within a macroscopic approach the potential barriers governing the entrance and decay channels of these  $4n$ -nuclei via alpha emission or absorption have also been compared.

The rms radii of the prolate chains seem incompatible with the experimental rms radii of the ground states. The binding energies of the three-dimensional molecules are higher than the binding energies of the planar shapes. The core+ $\alpha$  cluster system leads always to the lowest potential barrier. The binding energy can be obtained within the sum of the binding energy of  $n$  alphas plus 2.4 MeV multiplied by the number of bonds or by the sum of the binding energy of one alpha and the one of the daughter nucleus plus the Coulomb energy and the proximity energy between the two nuclei.

## References

- [1] W. von Oertzen, M. Freer, and Y. Kanada-En'yo, *Phys. Rep.* **432** (2006) 43.
- [2] D.J. Marin-Lambarri *et al.*, *Phys. Rev. Lett.* **113** (2014) 012502.
- [3] E. Epelbaum *et al.*, *Phys. Rev. Lett.* **112** (2014) 102501.
- [4] R. Bijker and F. Iachello, *Phys. Rev. Lett.* **112** (2014) 152501.
- [5] Y. Funaki *et al.*, *Phys. Rev. C* **80** (2009) 064326.
- [6] T. Suhara, Y. Funaki, B. Zhou, H. Horiuchi, and A. Tohsaki, *Phys. Rev. Lett.* **112** (2014) 062501.
- [7] G. Royer, B. Remaud, *Nucl. Phys. A* **444** (1985) 477.
- [8] G. Royer, M. Jaffré, and D. Moreau, *Phys. Rev. C* **86** (2012) 044326.
- [9] G. Royer, A. Escudie, and B. Sublard, *Phys. Rev. C* **90** (2014) 024607.
- [10] Y. Kanada-En'yo, *Prog. Theor. Phys.* **117** (2007) 655.
- [11] M. Chernykh *et al.*, *Phys. Rev. Lett.* **98** (2007) 032501.
- [12] E. Epelbaum *et al.*, *Phys. Rev. Lett.* **109** (2012) 252501.